

Modeling and Control of Magnetic Bearings with Nonlinear Magnetization (Simulation vs Experiment)

Ali GERAMI*, Roger FITTRO* and Carl KNOSPE*

*Department of Mechanical and Aerospace Engineering, University of Virginia,

122 Engineer's Way, Charlottesville, Virginia 22903, USA

E-mail: ag4n@virginia.edu, rff9w@virginia.edu, crk4y@virginia.edu

Abstract

This paper is a continuation of the work presented in (Gerami, et al., 2015), which explored the use of the Lur'e formulation to achieve increased dynamic load capacity in active magnetic bearings (AMBs). The increase in the load capacity was achieved by developing a nonlinear model that enabled the system to operate in the nonlinear region of the magnetization curve. While the previous work focused on the theoretical development of the modeling and control approach, this paper verifies the results by experiments conducted on a rocking beam test rig. The experiment demonstrates that the proposed modeling and control approach significantly improves the transient response and disturbance rejection capabilities of the magnetic bearing system compared with present industrial practice. Based on the excellent agreement between simulation and experimental results, it is shown that existing industrial AMBs could be modified to be significantly more resilient to unknown external disturbances, and therefore result in fewer shutdowns and less associated damage to backup bearings. In addition, for new AMB applications, smaller AMBs could be designed using this method which would be able to handle the same worst-case disturbance forces as larger AMB systems based on standard modeling and control methods.

Keywords : Magnetic Bearing, Nonlinear Modeling, Lur'e Formulation Linear Matrix Inequalities, Disturbance Rejection, Transient Response

1. Introduction

Active magnetic bearings (AMBs) are currently employed in significant numbers in industrial turbomachinery. Conventional practice is to develop controllers for the rotor system supported by these nonlinear actuators by first performing a linearization of the plant around a fixed operating point. This paper advocates a different approach presented in (Gerami, et al., 2015) where a Lur'e model of the bearing nonlinearities is employed. The goal of this investigation is the experimental verification of the improvement of transient response and disturbance rejection by allowing the feedback control to effectively operate even when the core material of the electromagnet experiences flux densities approaching magnetic saturation.

A number of previous investigations have examined the control of nonlinear AMB systems. These efforts can be categorized on the basis of the nonlinearity involved and the controller synthesis approach employed.

AMB Nonlinearities: A number of physical phenomena give rise to the nonlinearities present in magnetic bearings. The nature of force generation in an AMB system is fundamentally nonlinear even before any non-idealities of the actuator or drive electronics are considered. In addition to this nonlinearity, there are other important nonlinear elements in AMB systems (Ji, et al., 2008):

1. Nonlinear magnetization of the ferromagnetic core material, including magnetic saturation at high values of coil current;
2. Saturation of the power amplifier current and limits to its slew rate that result from the operational capabilities of the power amplifier as well as the coil inductance (Maslen, et al., 1989)

3. Coupling between electromagnet flux paths that arise from stator geometry.

The first and second nonlinearities have the most significant effect on the actuator force limit and are considered during the controller synthesis procedure presented in this paper.

Control Design Approach: Many research efforts have examined nonlinear control of AMBs. These approaches can be broadly placed into four categories depending on how the nonlinearity is treated during control system design: (1) the nonlinearity is not modeled but instead is accommodated in design via robustness to norm-bounded uncertainty (i.e., small gain approach); linear controller synthesis is carried out via robust control techniques such as μ -synthesis (Nonami and Ito, 1996, Fittro and Knospe 2002, Lanzon and Tsiotras, 2005); (2) the nonlinearity is characterized via its sector bounds (i.e., absolute stability approach); linear controller synthesis is carried out via linear matrix inequalities (LMIs) (Hu, et al., 2002, 2003, Fang, et al., 2004, Sanbayashi, et al., 2015, Gerami, et al., 2015); (3) the nonlinearity is ‘removed’ via feedback linearization (Lindlau and Knospe, 2002, Hsu and Chen, 2002, Li, et al., 2003, Franco, et al., 2005), so as to enable the use of linear control tools for the synthesis of a linear feedback controller; and (4) the nonlinearity remains unaltered; controller design techniques for nonlinear systems (e.g., backstepping (Queiroz, et al., 2005), sliding mode control (Cho, et al., 1993, Tian, et al., 1996, Rundell, et al., 1996, Lee, et al., 2003, Chen and Lin, 2011), are directly employed on the nonlinear plant. In this paper the second approach is examined. Specifically, we seek to design controllers that are effective when the electromagnetic actuators are operating close to the saturation flux density of the ferromagnetic materials used. This is done by treating the nonlinear magnetization as a Lur’e problem and developing LMIs for stability and performance of the closed loop system.

Lur’e Systems: A Lur’e system is a feedback interconnection of a linear time-invariant system and memoryless, possibly time-varying nonlinear block diagonal element that satisfies sector-bound conditions (refer to Figure 1). Only a few investigations have used a Lur’e systems approach for the nonlinearities related to magnetic bearing systems. LMI techniques were used to synthesize AMB controllers for systems with gyroscopics (Sanbayashi, et al., 2015) actuator saturation (Hu, et al., 2002, Fang, et al., 2004), and state constraints (Hu, et al., 2003). In this study, the Lur’e system approach to controller design for optimized transient and disturbance rejection performance as developed in (Gerami et al., 2015) is experimentally evaluated on a single degree-of-freedom AMB test rig. The remainder of the paper is organized as follows. In Section 2 the experimental test rig is presented. The modeling method is explained briefly in Section 3, Experimental results are presented in Section 4 and Section 5 concludes the paper.

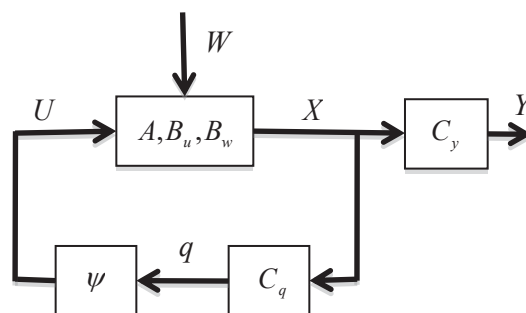


Figure 1: The Lur’e Problem Interconnection

2. Experimental test rig

A rocking beam test rig is used for modeling, simulation and experimental verification purposes (see Figure 2). The dynamic portion of the rig consists of a beam mounted on a single DOF pivot and 3 electromagnets: two control electromagnets (one at each end of the beam) and one disturbance electromagnet used to impose disturbance forces on the beam. The beam rotates about the knife-edge pivot and the control electromagnets produce the necessary forces to stabilize the beam. This experimental setup’s dynamics are simple; however, they include all of the fundamental features of an industrial magnetic bearing system. The rocking beam test rig system parameters are summarized in Table 1.

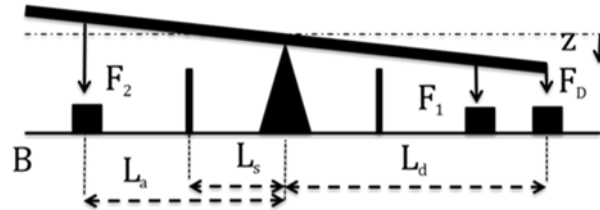
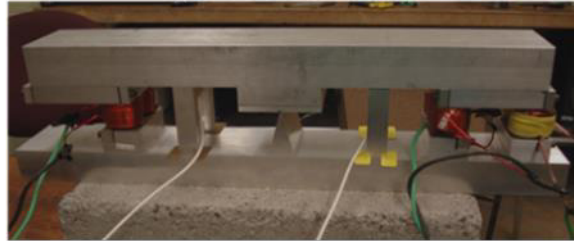


Figure 2: Rocking beam test rig

Table 1 Rocking beam parameters

Symbol	Specification	Value	Unit
J	Moment of inertia	153.33	gm^2
L_a	Control electromagnet distance	0.1556	m
L_{se}	Sensor distance	0.0889	m
L_d	Disturbance Distance	0.2302	m
L_{beam}	Beam Length	0.4731	m
g_0	Nominal gap width	0.762	mm
A	Pole face area	161.3	mm^2

3. Modeling

The dynamics of the test rig can be modeled by the following differential equation:

$$J\ddot{\theta} = L_a F_a + L_d F_d \quad (1)$$

$$F_a = k_s \theta + f(I_c) \quad (2)$$

where J is the moment of inertia of the beam, θ is the angle between the beam and the horizontal axis, F_a is the net force of the control actuators on the beam, F_d is the disturbance electromagnet force, L_a is the distance between the control electromagnets and the pivot, and L_d is the distance between the disturbance electromagnet and the pivot, k_s is the actuator open-loop stiffness, which can be obtained by linearizing the force around its equilibrium point. $f(I)$ is the force of the magnetic actuator assuming no displacement. In terms of the Lur'e problem, $f(I)$ is the nonlinear input function (ψ from Figure 1) and should therefore satisfy a sector condition:

$$k_1 I < f(I) < k_2 I \quad (3)$$

The sector bounds are lines with constant slopes of k_1 and k_2 (refer to Figure 3).

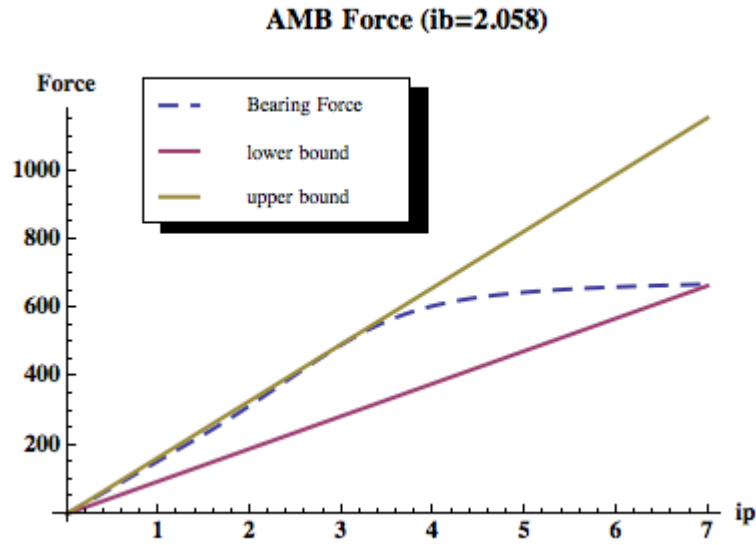


Figure 3: Sector Condition

Traditionally the magnetic bearing actuator force is calculated using the following equations:

$$F = \frac{A}{\mu_0} B^2 \quad (4)$$

$$B = \frac{\mu_0 NI}{2g} \quad (5)$$

where B is the flux density of the electromagnetic circuit, A is the cross sectional area of the core material, μ_0 is the permeability of free space, N is the number of turns in the coil, I is the coil current and g is the gap between the two parts of the core material (stator and rotor). However, for large flux densities, the silicon iron magnetic reluctance is significant and should therefore not be ignored as it is in Eq. (5). By considering this extra reluctance term, the magnetic flux density can be calculated as:

$$B = \frac{\mu_0 NI}{\frac{2g}{\mu_0} + \frac{L_s}{\mu_r}} \quad (6)$$

in which L_s is the length of silicon iron in the magnetic circuit and μ_r is the relative permeability of the silicon iron, which is a function of the flux density itself. Based on Eq. (6), the nonlinear actuator force can be calculated and substituted into the system level dynamic equations (Eq. 1 and 2) [Gerami et al. 2015].

Constraints on the physical operation of the magnetic bearing system were also taken into account in the modeling and control synthesis procedure performed in this work. The operational limits included are: 1) the angular movement of the beam, which is physically limited by the back-up bearings, and 2) the actuator currents, which are limited by the wire gauge and amplifier capabilities:

$$|\theta| \leq \theta_{\max} \quad (7)$$

$$0 < I_1, I_2 < I_b + I_{\max} \quad (8)$$

where I_{\max} is the limit on the control current I_c .

Details of the full derivation of the dynamic system equations, the conversion of the problem into the Lur'e format, inclusion of the system constraints and the formulation of the associated LMI can be found in (Gerami, et al., 2015).

4. Results (Simulation vs. Experimental Results)

The control synthesis procedure for optimized transient response and disturbance rejection performance discussed in detail in (Gerami, et al., 2015) was used to design and implement both Classical Jacobian Linearization (JL) and Lur'e Description (LD) controllers for the rocking beam test rig.

Transient Response: As can be seen from Figure 4, the resulting LD controller shows a significant transient response improvement over the conventional JL controller. The LD controller exhibits a rise time, which is 17% faster than the JL controller.

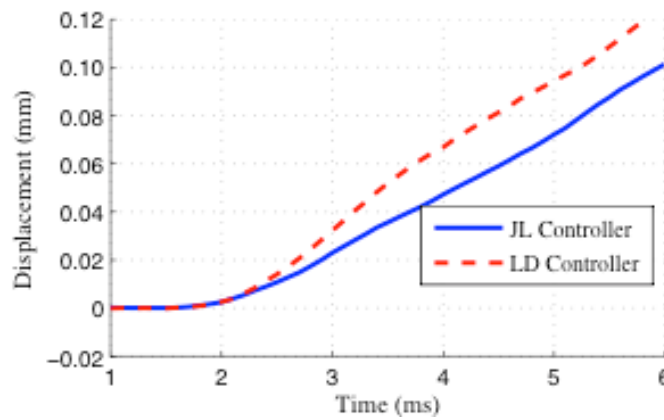


Figure 4: Experimental transient response to a 0.1mm (4mils) step comparing controllers based on Jacobian linearization (JL) and Lur'e Description (LD) formulation

Disturbance Rejection: The maximum guaranteed disturbance energy index (α_m) that the JL and LD controllers were found to be able to tolerate were 10 and 43 N^2s , respectively. Following controller synthesis, these controllers were implemented on the experimental setup.

A controlled external disturbance was imposed on the beam by using the disturbance electromagnet, situated toward the far end of one side of the rocking beam. Different pulse disturbance inputs were devised for testing the closed loop system, with energy indices of 10 N^2s and 43 N^2s . The durations and amplitudes of these disturbance inputs are summarized in Table 2.

Table 2 Disturbance force, duration, and energy index

	Disturbance 1	Disturbance 2	Disturbance 3	Disturbance 4	Disturbance 5	Disturbance 6
Duration(s)	0.01	0.05	0.1	0.01	0.05	0.1
Force (N)	31.6	14.1	10	65.6	29.3	20.7
Energy Index (N^2s)	10	10	10	43	43	43

The JL and LD controllers were tested with all pulse disturbances listed in Table 2, and the experimental results were compared with simulation predictions. As an example, the JL and LD controllers' responses to an impulse with an energy index of 43 N^2s and a duration of 0.1s are depicted in Figure 5 and 6. The simulation and experimental data are in very good agreement. In addition, the LD controller significantly improves the system's response to an external disturbance (by a factor of 4).

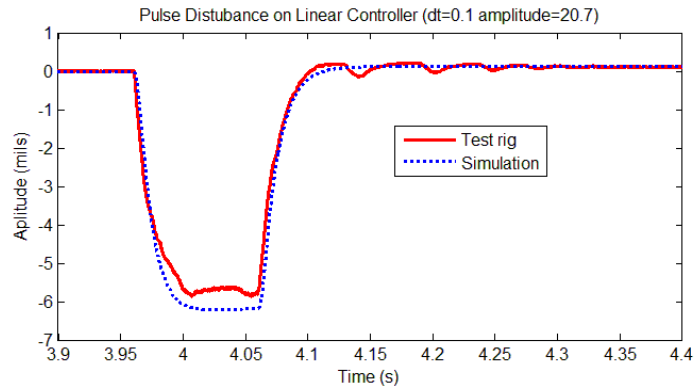


Fig. 5: Response to disturbance force of 20.7N with a duration of 0.1s (Jacobian Linearized model based control design)

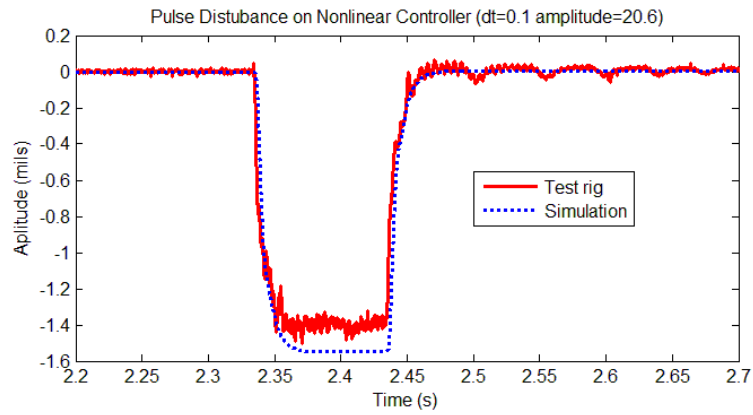


Fig. 6: Response to disturbance force of 20.7N with a duration of 0.1s (Lur'e Description model based control design)

Figure 7 compares the JL and LD controller responses to all pulse disturbances from Table 2 with an energy index of $43 \text{ N}^2\text{s}$. In all experiments, the displacements were recorded at the sensor location where the gap between the sensor stand and the beam is 0.38mm (15 mils). As can be seen from Figure 7, an impulse with the energy index of $43 \text{ N}^2\text{s}$ ($\Delta t = 0.01\text{s}$) drove the beam using the JL controller to impact the sensor stand. The same disturbance impulse moved the beam using the LD controller just under 0.15mm (6 mils), which is a 2.5x improvement.

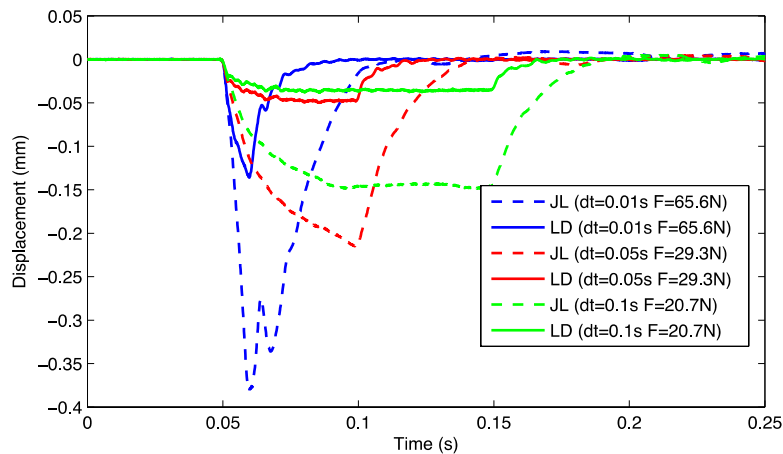


Figure 7: System responses to external disturbances with energy index of $43 \text{ N}^2\text{s}$

5. Conclusion

Based on the results obtained from the rocking beam test rig, the following conclusions can be drawn:

- By following a rigorous experimental model and parameter identification procedure, excellent correlation was obtained between the experimental data and theoretical predictions.
- In comparison to Jacobean linearized control design, a significantly improved transient response was achieved through the use of the proposed modeling and control design procedure. This was demonstrated by a 17% faster rise time.
- In comparison to Jacobean linearized control design, significant performance improvement in the form of a higher dynamic load capacity was achieved through the use of the proposed nonlinear modeling and LMI method for control synthesis. This was exemplified by the ability of the system to dissipate impulse disturbances with 4 times the energy compared with that achievable by a traditional control design.
- The main contribution of this work can be summarized as: A combined approach for modeling and control of magnetic bearings that optimally uses the extra load capability within the nonlinear magnetization region was developed and experimentally verified. Based on these results, existing industrial AMBs could be modified to be significantly more resilient to unknown external disturbances. And for new AMB applications, smaller AMBs could be designed which would be able to handle the same worst-case disturbance forces as larger existing AMB systems.

Acknowledgements

The authors would like to acknowledge the Rotating Machinery and Controls Laboratory at the University of Virginia, which supplied the funding for the worked described in this paper.

References

- Chen, S., & Lin, F. (2011), Robust Nonsingular Terminal Sliding-Mode Control for Nonlinear Magnetic Bearing System, *IEEE Transactions on Control Systems Technology*, 19(3), 636-643.
- Cho, Dan, Yoshifumi Kato, and Darin Spilman, Sliding Mode and Classical Controllers in Magnetic Levitation Systems, *IEEE Control Systems* 13.1 (1993): 42-48. Print.
- Fang, H., Lin, Z., & Hu, T. (2004), Analysis of linear systems in the presence of actuator saturation and L2-disturbances, *Automatica*, 40(7), 1229-1238.
- Fittro, R., & Knospe, C. (2002), Rotor compliance minimization via μ -control of active magnetic bearings, *IEEE Transactions on Control Systems Technology*, 10(2), 238-249.
- Franco, Ana Lucia D., Henri Bourles, and Edson R. De Pieri, A Robust Nonlinear Controller with Application to a Magnetic Bearing System, *Proc. of 44th IEEE Conference on Decision and Control, and the European Control Conference*, Seville, Spain, N.p.: n.p., 2005. 4927-932. Print.
- Gerami, A., Allaire, P., & Fittro, R. (2015), Control of Magnetic Bearing with Material Saturation Nonlinearity, *Journal of Dynamic Systems, Measurement, and Control*, 137(6), 061002.
- Hsu, C., & Chen, S. (2002), Exact linearization of a voltage-controlled 3-pole active magnetic bearing system, *IEEE Transactions on Control Systems Technology*, 10(4), 618-625.
- Hu, T., Lin, Z., & Chen, B. M. (2002). An analysis and design method for linear systems subject to actuator saturation and disturbance, *Automatica*, 38(2), 351-359.
- Hu, T., Lin, Z., Jiang, W., & Allaire, P. (2003), Constrained control design of magnetic bearing systems, *Proceedings of the 2003 American Control Conference*, 2003.
- Ji, J., Hansen, C. H., & Zander, A. C. (2008), Nonlinear Dynamics of Magnetic Bearing Systems, *Journal of Intelligent Material Systems and Structures*, 19(12), 1471-1491.
- Lanzon, A., & Tsiotras, P. (2005). A combined application of Hinf loop shaping and mu-synthesis to control high-speed flywheels, *IEEE Transactions on Control Systems Technology*, 13(5), 766-777.
- Lee, J., Allaire, P., Tao, G., Decker, J., & Zhang, X. (2003), Experimental study of sliding mode control for a

- benchmark magnetic bearing system and artificial heart pump suspension, *IEEE Transactions on Control Systems Technology*, 11(1), 128-138.
- Li, L., Shinshi, T., & Shimokohbe, A. (2003). Asymptotically exact linearizations for active magnetic bearing actuators in voltage control configuration, *IEEE Transactions on Control Systems Technology*, 11(2), 185-195.
- Lindlau, J., & Knospe, C. (2002). Feedback linearization of an active magnetic bearing with voltage control, *IEEE Transactions on Control Systems Technology*, 10(1), 21-31.
- Maslen, E., Hermann, P., Scott, M., & Humphris, R. R. (1989), Practical Limits to the Performance of Magnetic Bearings: Peak Force, Slew Rate, and Displacement Sensitivity, *Journal of Tribology*, 111(2), 331.
- Nonami, K., & Ito, T. (1996). μ synthesis of flexible rotor-magnetic bearing systems, *IEEE Transactions on Control Systems Technology*, 4(5), 503-512.
- Queiroz, M. D., & Dawson, D. (1996). Nonlinear control of active magnetic bearings: A backstepping approach, *IEEE Transactions on Control Systems Technology*, 4(5), 545-552.
- Rundell, A., Drakunov, S., & Decarlo, R. (1996), A sliding mode observer and controller for stabilization of rotational motion of a vertical shaft magnetic bearing, *IEEE Transactions on Control Systems Technology*, 4(5), 598-608.
- Sanbayashi, A., Narita, M., Chen, G., & Takami, I. (2015), Gain scheduled control for active magnetic bearing system considering gyroscopic effect, 2015 7th International Conference on Information Technology and Electrical Engineering (ICITEE).
- Tian, Hongqi, and Kenzo Nonami, Discrete-time Sliding Mode Control of Flexible Rotor-magnetic Bearing Systems, *International Journal of Robust and Nonlinear Control* 6.7 (1996): 609-32.